Attitude Tracking of the Small-Scale Helicopter System using Disturbance Observer based Sliding Mode Control

Almir Salihbegovic, Mujo Hebibovic
Department for Automatic Control and Electronics
Faculty of Electrical Engineering, University of Sarajevo
71000 Sarajevo, Bosnia and Herzegovina
almir.salihbegovic@etf.unsa.ba

Abstract— **Control design for a small-scale helicopter is quite challenging due to its nonlinearities, unknown and unmodelled dynamics, strong cross-coupling effects produced by the vehicles actuators, parametric uncertainties and external disturbances. This paper introduces the design of robust and stable disturbance observer (DOB) based sliding mode control (SMC) to meet these issues. It consists of the disturbance observer in the inner control loop which estimates and attenuates plant input generalized disturbance, and the sliding mode controller in the outer control loop which enforces convergence to the reference and stability of the equilibrium. Introduced disturbance observer is a linear low-pass filter capable to compensate unwanted chattering effects of the sliding mode control. The highly nonlinear helicopter model is introduced to illustrate effectiveness of the proposed control method. Designed controllers are implemented in the simulation mode and experimentally tested in a realistic environment. Obtained results showed that developed DOB based SMC controllers improve tracking performances over the entire range of the helicopter output variables even in the presence of additional parametric uncertainties, and external disturbances in the form of wind gusts.**

I. Introduction

Requirements for the high precision and accuracy operations of modern electromechanical systems become more and more strict. Advanced control techniques play significant role while meeting these challenges.

Helicopters are very suitable for a wide range of applications such as air surveillance, transportation, rescue, etc. They are also used as combat aerial vehicles. On the other hand, unstable behaviour in the open-loop, strong cross-coupling effects produced by the vehicle actuators, unknown and unpredictable inputs (disturbance and noise), unmodelled and unknown dynamics, parametric uncertainties and external disturbances appear to be the main difficulties in control of such systems. Therefore, the nonlinear helicopter modelling and control techniques have been intensively developed in the recent decades [1], [2].

Various control techniques have been applied to control elevation and azimuth angles of the helicopter system CE 150 supplied by Humosoft [3]–[6]. Model predictive control (MPC), linear quadratic optimal control combined with a state estimator (LQG), and optimal linear quadratic output control (PLQ) are applied to the helicopter system CE 150, and the comparative analysis is discussed in [5]. The proposed control schemes have resulted in improved tracking performances of the helicopter system in comparison with the classical control methods.

Further improvements in controlling nonlinear helicopter model CE 150 have been achieved using the artificial intelligence methods [3], [4]. Addressed control techniques do not practice estimation of the helicopter cross-coupling effects, disturbances and uncertainties, thus tracking performance and computational burden parameters are slightly degraded.

Disturbance observer (DOB) based control appeared in the late 1980s and thereafter it attracts considerable interests in the field of high performance positioning systems. The DOB based control is widely used in industry [7]–[11]. Many authors have studied effectiveness of disturbance observers in controlling helicopter systems [12], [13] and quadrator vehicles [14], [15]. Tracking performances of the helicopter system CE 150 are significantly improved using DOB based control described in [13].

This paper focuses high performance disturbance observer based sliding mode control of the helicopter system CE 150 in the presence of unknown and unmodelled dynamics, strong cross-coupling effects, parametric uncertainties and external disturbances. Introduced disturbance observers are linear low-pass filters capable to compensate unwanted chattering effects of the sliding mode control. Additional disturbance terms which represent wind gusts and 30% of additional uncertainties on model parameters are applied to demonstrate control performance. It will be shown that proposed cascade control structure provides robust stability and superior tracking performance even in the presence of additional parametric uncertainties and external disturbances.

The paper is organized as follows. In Section II the control strategy and helicopter modelling are presented. The sliding mode controller for precise position tracking is developed in Section III. Also, the disturbance observer based on position measurements and control input is also designed in this section. Simulation and experimental results are discussed in Section IV. Concluding remarks are given in Section V.

II. Control strategy and helicopter modelling

As Fig. 1 shows, the overall control structure is composed of three central parts: the PC based controllers, the interface module and the helicopter system. Attitude controllers of

the helicopter system are designed in MATLAB/Simulink. The multifunctional card MF624 is used as interface module between the helicopter system and PC based controllers. It facilitates data acquisition and transmission with MATLAB Real Time Toolbox. Real time experiments are performed using MATLAB xPC Target Toolbox. The helicopter system Humosoft CE 150 is presented in Fig. 2. It is composed of the rigid body, two DC motors with permanent stator magnets that drive main and tail rotors, power amplifiers and encoders as sensors. In the following paragraphs the simplified helicopter model will be presented.

A. Helicopter modelling

In this subsection only the main results of the helicopter CE 150 modelling are presented. The derivation process of its complete dynamics is too long and can be found in [16]. The helicopter system CE 150 (supplied by Humosoft) has two degrees of freedom: elevation (pitch) angle ψ that represents rotation around horizontal axis, and azimuth (jaw) angle φ that represents rotation around vertical axis. The helicopter model is the nonlinear MIMO system with two inputs (voltage of the main motor u_1 and voltage of the tail motor u_2) and two outputs (elevation angle ψ and azimuth angle φ). The operating ranges of the helicopter output signals are: $\psi \in [-45^\circ, 45^\circ]$ and $\varphi \in [-130^\circ, 130^\circ]$. The elevation dynamics considers the torques in the vertical plane yielding the equations:

$$a_\psi \ddot{\psi} = \tau_1 + \tau_{\dot{\varphi}} - \tau_{f_1} - \tau_m + \tau_G, \tag{1}$$

$$\tau_m = mgl \sin\psi, \tag{2}$$

$$\tau_{\dot{\varphi}} = ml\dot{\varphi}^2 \sin\psi \cos\psi, \tag{3}$$

$$\tau_{f_1} = C_\psi \text{sign}\,\dot{\psi} + B_\psi \dot{\psi}, \tag{4}$$

$$\tau_G = k_G \dot{\varphi} \omega_1 \cos\psi, \text{ for } \dot{\varphi} \ll \omega_1. \tag{5}$$

Here, a_ψ is the moment of inertia around the horizontal axis, τ_1 stands for the moment produced by the main motor propeller, $\tau_{\dot{\varphi}}$ is the centrifugal torque, τ_{f_1} represent Coulumb and viscous friction torques, τ_m is the gravitation torque, τ_G is the gyroscopic torque, m is the helicopter body mass, g is the gravitational acceleration, l is the distance from the vertical axis to main motor axis, ω_1 is the main propeller angular velocity, B_ψ and C_ψ represent viscous and Coulumb friction coefficients, respectively, and k_G is the gyroscopic coefficient. Equations (1)−(5) do not consider the main propeller speed influence to the elevation friction torque, and air resistance variation that depends on the main propeller angular velocity. All these unmodelled influences will be estimated by the disturbance observer design. Considering the torques in the horizontal plane, the azimuth dynamics is presented with the following equations [16]:

$$a_\varphi \ddot{\varphi} = \tau_2 - \tau_{f_2} - \tau_r, \tag{6}$$

$$\tau_{f_2} = C_\varphi \text{sign}\,\dot{\varphi} + B_\varphi \dot{\varphi}, \tag{7}$$

$$a_\varphi = a_\psi \sin\psi, \tag{8}$$

where a_φ is the moment of inertia around vertical axis, τ_2 is the moment produced by the tail motor propeller, τ_{f_2} represent Coulumb and viscous friction torques, τ_r is the reaction torque of the main motor, B_φ and C_φ stand for viscous and Coulumb friction coefficient, respectively, and ω_2 is the angular velocity of the tail propeller. The tail propeller speed influence to the azimuth friction torque has not been introduced in (7) and will be compensated with the disturbance observer design.

B. DC motor and propeller dynamics modelling

The main DC motor dynamics can be presented by the second order transfer function [16]:

$$\frac{\omega_1(s)}{u_1(s)} = \frac{1}{(T_1 s + 1)^2}, \tag{9}$$

where $\omega_1(s)$ and $u_1(s)$ are Laplace transforms of $\omega_1(t)$ and $u_1(t)$, respectively, and T_1 is the main motor time constant. The parabolic function of the angular velocity is used to describe the main propeller torque [16]:

$$\tau_1(t) = a_1 \omega_1^2(t) + b_1 \omega_1(t), \tag{10}$$

where a_1 and b_1 are parameters of the main propeller characteristic. The parameters T_1, a_1, b_1 are considered in the identification process. Analogue relations to (9) and (10) can be written for the tail DC motor, replacing T_2, a_2, b_2 with T_1, a_1, b_1.

C. DC motors cross-coupling model

Strong cross-coupling effects between the elevation and azimuth dynamics are the major composite feature of the helicopter system. Reaction torque of the main motor to the tail motor is presented by the first order transfer function [16]:

$$\frac{\tau_r(s)}{u_1(s)} = K \frac{T_z s + 1}{T_p s + 1}. \tag{11}$$

Unknown helicopter parameters are determined using a simple genetic algorithm with reduced number of conducted experiments as in [17]. Values of the helicopter parameters used for the simulation model synthesis are listed in [13].

III. Synthesis of the DOB based SMC control

This section describes synthesis of the disturbance observer based sliding mode control of the helicopter system presented in the previous section. The control task specification includes: closed-loop system stability, reference signal tracking, and reduced influence of parametric uncertainties, disturbances and unmodelled dynamics.

A single degree of freedom mechanical system (either translational or rotational) can be described with the second order differential equation [18]:

$$a(q)\ddot{q}(t) + \tau_d\left(q(t), \dot{q}(t), t\right) = \tau, \tag{12}$$

where q and $\dot{q} \equiv v$ stand for the state variables, position and velocity, respectively, $a(q)$ is bounded inertia of the system and τ_d is bounded plant input disturbance that includes Coriolis torques (forces), friction torque, gravitational torque and external torques. Also, the acceleration and the control torque are assumed bounded for the system (12).

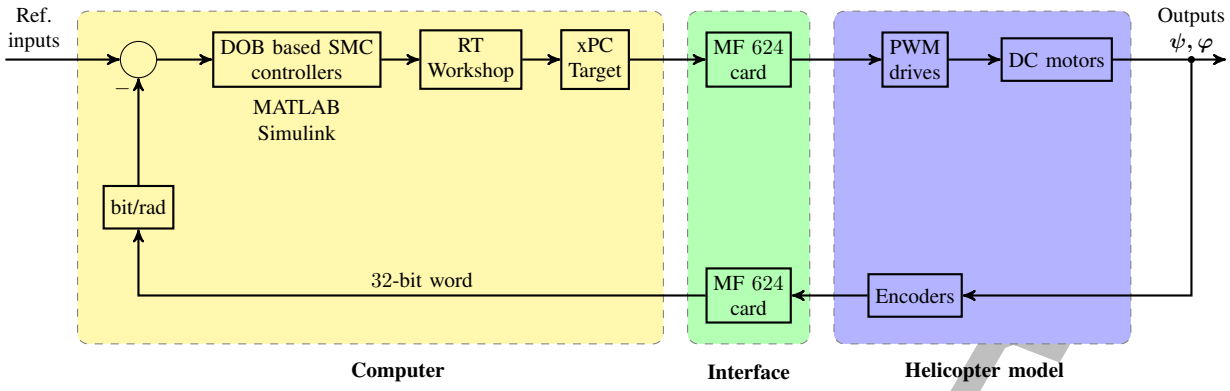

Fig. 1. Block diagram of the proposed real-time control system for the helicopter model

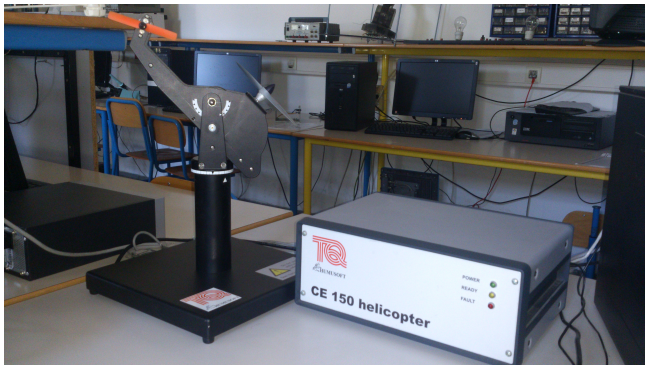

Fig. 2. Helicopter system CE 150

If the nominal inertia coefficient a_N is known, varying inertia $\Delta a(q)$ can be represented as $\Delta a(q) = a(q) - a_N$ and lumped into the generalized system input disturbance $\tau_{dis} = \tau_d + \Delta a(q)\ddot{q}$, so the system (12) yields:

$$a_N \ddot{q}(t) + \tau_{dis}(q(t), \dot{q}(t), t) = \tau. \quad (13)$$

The elevation dynamics (1) can be presented with (13), introducing identities: $a_N \equiv a_\psi$, $q \equiv \psi$, $\tau_{dis} \equiv \tau_{f1} + \tau_m - \tau_{\dot{\psi}} - \tau_G$ and $\tau \equiv \tau_1$. Also, the azimuth dynamics (7) can be described with (13), substituting: $a_N \equiv a_\varphi$, $q \equiv \varphi$, $\tau_{dis} \equiv \tau_{f2} + \tau_r$ and $\tau \equiv \tau_2$. The main idea consists of forming the control law as follows:

$$\tau = a_N \ddot{q}_{des} + \hat{\tau}_{dis}. \quad (14)$$

The control input (14) has two components, the torque $a_N \ddot{q}_{des}$ induced by desired acceleration, and the estimated generalised disturbance $\hat{\tau}_{dis}$. The control torque (14) included in (12) cancels plant input generalized disturbance and makes system a simple double integrator $\ddot{q} = \ddot{q}_{des}$, thus, robust according to parametric uncertainties and disturbances. Fig. 3 shows the proposed cascade control structure that implements the control input (14) to the system (12).

A. Synthesis of the outer control loop

Assume that the control output is continuous function of position $y(q)$. The tracking error $e(q,t) = y(q) - y_{ref}(t)$ is a measure of the distance from the output $y(q)$ to its reference value y_{ref}. If the tracking error is equal to zero, system output is constrained to the manifold (domain):

$$S = \left\{ q, t \middle| e(q,t) = y(q) - y_{ref}(t) = 0 \right\}. \quad (15)$$

Now, the control task can be defined as requirement to enforce convergence to the manifold (15), or to enforce the equilibrium $e(y, y_{ref}) = 0$ and stability of the equilibrium. The generalized error $\sigma = \sigma(e, \dot{e})$ is introduced to provide relative degree one with respect to control input:

$$\sigma(e, \dot{e}) = \dot{e} + k_1 e, \quad (16)$$

where k_1 is a positive constant. The desired acceleration $\ddot{q}_{des}$ needs to guarantee convergence of the output to its reference and stability of the equilibrium. It consists of the equivalent and the convergence acceleration, namely:

$$\ddot{q}_{des} = \ddot{q}_{eq} + \ddot{q}_{con}. \quad (17)$$

The equivalent acceleration $\ddot{q}_{eq}$ is selected to guarantee zero rate of change of the distance from the equilibrium if the initial conditions are consistent with the equilibrium $\sigma|_{t=0} = 0$. The convergence acceleration provides convergence to the equilibrium solution if the initial conditions are not consistent with the equilibrium $\sigma|_{t=0} \neq 0$. The convergence acceleration should fade $\ddot{q}_{conv} = 0$ if equilibrium is reached $\sigma = 0$ and the desired acceleration is equal to the equivalent acceleration $\ddot{q}_{des} = \ddot{q}_{eq}$. Also, the desired acceleration must be equal to the convergence acceleration $\ddot{q}_{des} = \ddot{q}_{con}$ if the equilibrium solution is not reached, thus the influence of the equivalent acceleration $\ddot{q}_{eq}$ should vanish for $\sigma \neq 0$ [18].

The generalized error dynamics is calculated according to (15) and (16):

$$\dot{\sigma} = \frac{\partial y}{\partial q}\left(\ddot{q} - \left(\frac{\partial y}{\partial q}\right)^{-1}\left(\ddot{y}_{ref} - \frac{\partial^2 y}{\partial q^2}\dot{q}^2 - k_1 \dot{e}\right)\right). \quad (18)$$

Using $\dot{\sigma} = 0$ and (18) the equivalent acceleration can be expressed as:

$$\ddot{q}_{eq} = \left(\frac{\partial y}{\partial q}\right)^{-1}\left(\ddot{y}_{ref} - \frac{\partial^2 y}{\partial q^2}\dot{q}^2 - k_1 \dot{e}\right). \quad (19)$$

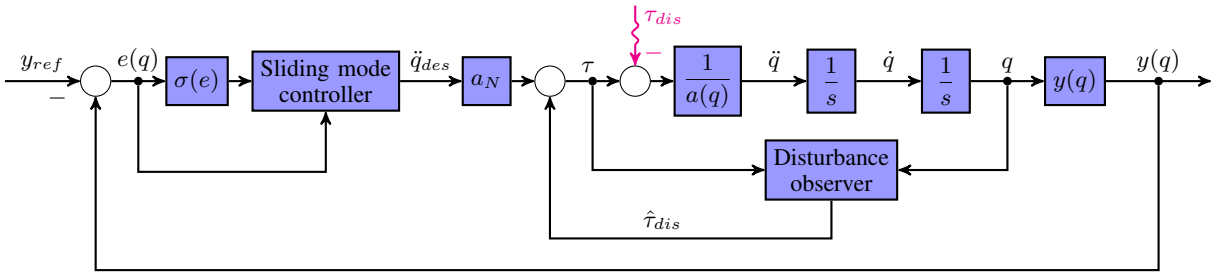

Fig. 3. Cascade control structure with DOB in the inner loop and SMC in the outer loop

The convergence acceleration yields from (18):

$$\ddot{q}_{con} = \left(\frac{\partial y}{\partial q}\right)^{-1} \dot{\sigma}. \tag{20}$$

The generalized error rate of change $\dot{\sigma}$ needs to be determined in order to complete design of the convergence acceleration. To this end, Lyapunov function candidate can be selected as:

$$V = \frac{\sigma^2}{2} > 0,\ V(0) = 0. \tag{21}$$

In order to guarantee boundedness of the control input τ for the system (12) and finite time convergence to the equilibrium $\sigma = 0$, the first order time derivative of the Lyapunov function (21) can be selected as:

$$\dot{V} = \sigma\dot{\sigma} = -k2^{\alpha}V^{\alpha},\ \frac{1}{2} \leq \alpha < 1, \tag{22}$$

where k is a positive Lyapunov coefficient that represents convergence rate. The exponential convergence is provided for $\alpha = 1$ and discussed in our previous paper [13]. Relations (21) and (22) yield:

$$\sigma\left(\dot{\sigma} + k\sigma^{2\alpha-1}\right) = 0. \tag{23}$$

The exponent $2\alpha - 1$ is bounded and lies within interval $[0, 1)$. The expression (23) may yield imaginary solutions if $\sigma < 0$. For the simplicity, the following analysis will consider only values of α that provide real values for $\sigma^{2\alpha-1}$ and satisfy:

$$\sigma^{2\alpha-1} = |\sigma|^{2\alpha-1}\,\mathrm{sign}(\sigma). \tag{24}$$

The convergence acceleration depends on the generalized error rate of change and can be expressed using (20), (23) and (24):

$$\ddot{q}_{con} = -k\left(\frac{\partial y}{\partial q}\right)^{-1} |\sigma|^{2\alpha-1}\,\mathrm{sign}(\sigma). \tag{25}$$

The sign of the convergence acceleration (25) is opposite to the sign of the distance from the equilibrium, thus directing motion towards the equilibrium solution $\sigma = 0$. Specially, for $\alpha = \frac{1}{2}$ the desired acceleration takes a specific form:

$$\ddot{q}_{des} = \left(\frac{\partial y}{\partial q}\right)^{-1}\left(\ddot{y}_{ref} - \frac{\partial^2 y}{\partial q^2}\dot{q}^2 - k_1\dot{e} - k\mathrm{sign}(\sigma)\right). \tag{26}$$

Motion generated by the control input (26) is followed with the high frequency oscillations around equilibrium and is known as sliding mode motion [18]. The chattering effect of the sliding mode control (27) will be partially compensated with the disturbance observer design in the form of linear low-pass filter.

If the position q is selected as output variable $y(q)$, i.e. $y(q) = q$, the desired acceleration for the helicopter control purpose is calculated using (26):

$$\ddot{q}_{des} = \ddot{y}_{ref} - k_1\dot{e} - k\,\mathrm{sign}\,(\sigma)\,. \tag{27}$$

Controller parameters k and k_1 are designed according to the nominal system selected to represent a simple double integrator $P_n(s) = \frac{1}{s^2}$. The coefficients $k_\psi = 4$ and $k_\varphi = 1$ are applied, so the elevation and azimuth angles tend to reference inputs as quickly as possible. Also, when the coefficients $k_{1\psi} = 1.8$ and $k_{1\varphi} = 4$ are applied, the elevation and azimuth overshoots are as small as possible.

B. Synthesis of the inner control loop

The disturbance observer design based on position measurements q, known nominal inertia coefficient a_N and control torque τ will be discussed in this subsection.

We will assume that the disturbance can be modelled as the output of a linear system with unknown initial conditions, thus it can be represented by a polynomial of time. The system (13) augmented with the disturbance model $\dot{\vartheta} \approx 0$, $\vartheta = -a_N^{-1}\tau_{dis}$ is observable [18]. Intermediate variables z_1 and z_2 can be selected as:

$$z_1 = \vartheta - l_1 q,\ l_1 = const, \tag{28}$$

$$z_2 = \dot{q} - l_2 q,\ l_2 = const. \tag{29}$$

The first order time derivatives along the trajectories of the system (13) are:

$$\dot{z}_1 = -l_1\left(z_2 + l_2 q\right), \tag{30}$$

$$\dot{z}_2 = z_1 - l_2 z_2 + \left(l_1 - l_2^2\right)q + a_N^{-1}\tau. \tag{31}$$

The dynamics of the observer is supposed to be the same as dynamics of the intermediate variables:

$$\dot{\hat{z}}_1 = -l_1\left(\hat{z}_2 + l_2 q\right), \tag{32}$$

$$\dot{\hat{z}}_2 = \hat{z}_1 - l_2\hat{z}_2 + \left(l_1 - l_2^2\right)q + a_N^{-1}\tau. \tag{33}$$

Laplace transformation of (32) and (33), after solving for $\hat{z}_1$, yields:

$$\hat{z}_1 = -l_1\frac{l_2 sq + l_1 q + a_N^{-1}\tau}{s^2 + l_2 s + l_1}\,. \tag{34}$$

Integrating (34) in $\hat{\vartheta} = \hat{z}_1 + l_1 q$ follows:

$$\hat{\tau}_{dis} = \frac{l_1}{s^2 + l_2 s + l_1} \tau_{dis}. \tag{35}$$

The estimated disturbance represents output of the linear low-pass filter (35) with the cut-off frequency determined by the parameters l_1 and l_2. The selection of the filter cut-off frequency is not tuned for the best performance, but rather to illustrate properties of the disturbance observer. The values $l_{1\psi} = 0.6$, $l_{2\psi} = 1.7$ for the elevation dynamics, and $l_{1\varphi} = 1.2$, $l_{2\varphi} = 1.7$ for the azimuth dynamics are selected, so the observer may estimate cross-coupling interactions in the low frequency range, and chattering effects and noise in the high frequency range. Disturbance observers for the elevation and the azimuth dynamics provided reduction of the 2DOF helicopter system to two independent 1DOF systems, thus the SMC controllers synthesis is performed according to their nominal models. Implementation of the disturbance observer (35) is shown in Fig. 4.

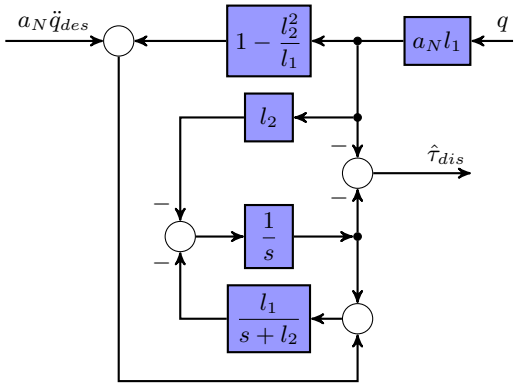

Fig. 4. Disturbance observer obtained from the desired acceleration and the position as inputs

IV. Simulation and Experimental Results

The simulation and the experimental results of the helicopter CE 150 control are presented in this section. The simulation model of the helicopter system was developed in Simulink according to section II. Various reference signals were tested, but step changes of the reference inputs are selected due to comparison with the results discussed in [13] and [3]. In all conducted simulations and experiments elevation and azimuth reference signals are simultaneous, and their step changes are smoothed due to the control input (27) that includes the second order time derivative of the reference signal.

A. Simulation results

Numerical simulations are first carried out in Simulink to investigate the robustness of the proposed control scheme. Presence of the additional external disturbances is assumed. The low-frequency sinusoidal signal $10\sin(0.5t)[m/s]$ and the high-frequency sinusoidal signal $10\sin(50t)[m/s]$ are added to both the elevation and the azimuth dynamics to represent wind gusts. These amplitudes are significantly strong for the tested small-scale helicopter system. Furthermore, 30% uncertainties on the model parameters are included as additional disturbances. In Fig. 5 it can be seen that the helicopter elevation maintains its reference value and stability of the equilibrium, even in the presence of significant additional external disturbances. The elevation tracking errors are shown in the Fig. 6 for better insight of the tracking quality. The proposed control exhibited superior tracking performances considering disturbances from both, internal and external sources, and maintain the helicopter position very well.

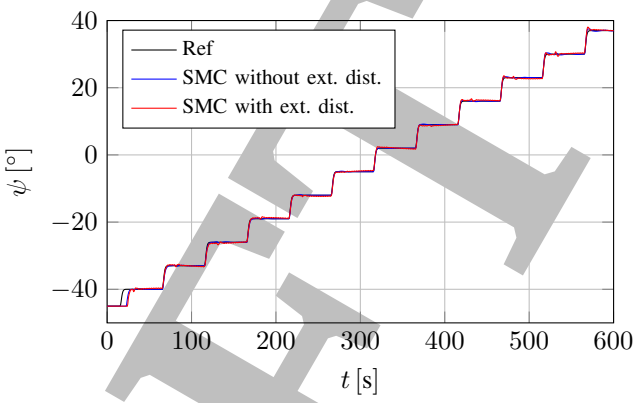

Fig. 5. Comparison of the elevation angle responses in the sim. mode

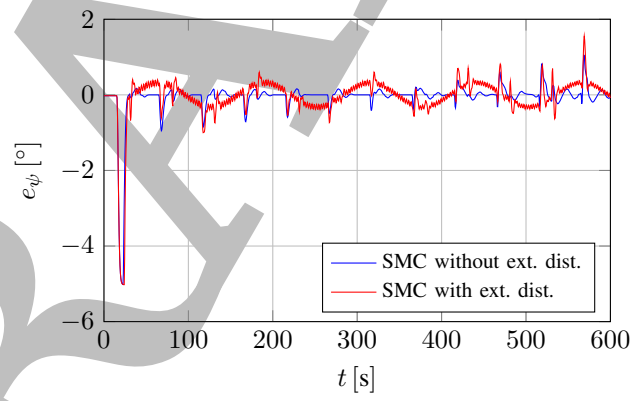

Fig. 6. Comparison of the elevation tracking errors in the sim. mode

B. Experimental results

This subsection presents improvements of the DOB based SMC control scheme through experiments, in comparison with DOB based framework developed in our previous paper [13]. The real helicopter system is required to track step changes in reference signals for the elevation and azimuth dynamics. The elevation angle response is shown in Fig. 7 and the azimuth angle response in Fig. 8. It can be noticed that both controllers are able to deal with parametric uncertainties and cross-coupling interactions, thus achieving satisfactory tracking performances over the entire range of elevation and azimuth angles. As Fig. 9 shows, lower overshoots and steady state errors are obtained with DOB based SMC control, especially approaching the maximum

value of the elevation angle. It can be noticed that disturbance observers efficiently compensate chattering effects of the sliding mode based controllers.

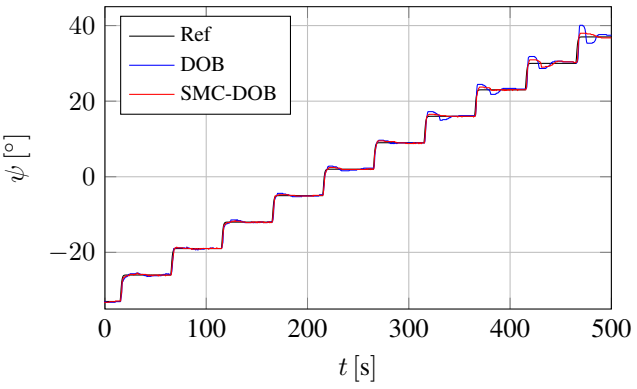

Fig. 7. Comparison of the elevation angle responses at the exp. setup

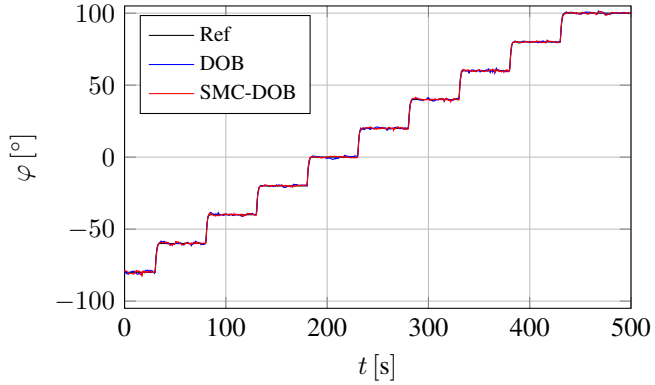

Fig. 8. Comparison of the azimuth angle responses at the exp. setup

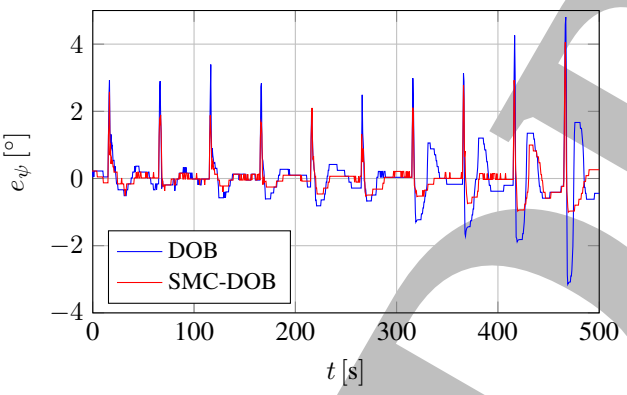

Fig. 9. Comparison of the elevation angle responses at the exp. setup

V. Conclusions

In this paper disturbance observer based sliding mode control is introduced and implemented to the nonlinear helicopter system CE 150. The porposed control achieved superior tracking performance even in the presence of unmodelled and unknown dynamics, nonlinear friction forces, parametric uncertainties, chattering effect and strong cross-coupling interactions of the elevation and the azimuth dynamics. Additional external disturbances with significant strong amplitudes that represent wind gusts, and 30% uncertainties on the model parameters are also added to the plant input generalized disturbance, to approve robustness of the proposed control scheme for entire range of the elevation and azimuth angles. The validity and improvements of the proposed cascade control structure was verified through both, simulation and experiment.

References

[1] A. Isidori and C. I. Byrnes, "Output regulation of nonlinear systems," in *IEEE Transactions on Automatic Control*, vol. 35, no. 2, Feb. 1990, pp. 131–140.

[2] T. J. Koo and S. Sastry, "Output tracking control design of a helicopter model based on approximate linearization," in *Proceedings of the 37th IEEE Conference on Decision and Control*, vol. 4, Dec. 1998, pp. 3635–3640.

[3] J. Velagic and N. Osmic, "Design and implementation of fuzzy logic controllers for helicopter elevation and azimuth controls," in *IEEE Conference on Control and Fault Tolerant Systems*, Nice, France, Oct 2010, pp. 311–316.

[4] J. Velagić and N. Osmić, "Identification and control of 2dof nonlinear helicopter using intelligent methods," in *IEEE Conference on System, Man and Cybernetics*, Istanbul, Turkey, 2010, pp. 2267–2275.

[5] J. Balderud and D. I. Wilson, "A comparison of optimal control strategies for a toy helicopter," in *Asian Control Conference*, Singapore, Sep 2002, pp. 1432 – 1437.

[6] ——, "Application of predictive control to a toy helicopter," in *IEEE International Conference on Control Applications*, Glasgow, Scotland, Sep 2002, pp. 1225–1229.

[7] H. S. Lee and M. Tomizuka, "Robust motion controller design for high accuracy positioning systems," in *IEEE Transactions on Industrial Electronics*, vol. 43, 1996, pp. 48–55.

[8] C. J. Kempf and S. Kobayashi, "Disturbance observer and feedforward design for a high-speed direct-drive positioning table," in *IEEE Transactions on Control System Technology*, vol. 7, 1999, pp. 513–526.

[9] B. K. Kim and W. K. Chung, "Advanced design of disturbance observer for high performance motion control systems," in *American Control Conference*, 2002, pp. 2112–2117.

[10] M. White, M. Tomizuka, and C. Smith, "Rejection of disk drive vibration and shock disturbances with a disturbance observer," in *IEEE American Control Conference*, vol. 6, 1999, pp. 4127 – 4131.

[11] X. Chen, S. Komada, and T. Fukuda, "Design of nonlinear disturbance observer," in *IEEE Transactions on Industrial Electronics*, vol. 47, 2000, pp. 429–437.

[12] B. Ahmed and F. Kendoul, "Flight control of a small helicopter in unknown wind conditions," in *Decision and Control (CDC), 2010 49th IEEE Conference on*, Dec 2010, pp. 3536–3541.

[13] A. Salihbegovic, E. Sokic, N. Osmic, and M. Hebibovic, "High performance disturbance observer based control of the nonlinear 2dof helicopter system," in *Information, Communication and Automation Technologies (ICAT), 2013 XXIV International Symposium on*, 2013, pp. 1–7.

[14] L. Besnard, Y. Shtessel, and B. Landrum, "Control of a quadrotor vehicle using sliding mode disturbance observer," in *American Control Conference, 2007. ACC '07*, July 2007, pp. 5230–5235.

[15] S.-H. Jeong and S. Jung, "Experimental studies of a disturbance observer for attitude control of a quad-rotor system," in *Control, Automation and Systems (ICCAS), 2012 12th International Conference on*, Oct 2012, pp. 579–583.

[16] P. Horáček, *CE 150 HELICOPTER MODEL, Educational manual*, Humosoft Ltd., Czech Republic, 2007.

[17] N. Osmic, J. Velagic, and S. Konjicija, "Genetic algorithm based identification of a nonlinear 2dof helicopter model," in *IEEE Mediterranean Conference on Control and Automation*, Marrakech, Morocco, 2010, pp. 333–338.

[18] A. Šabanović and K. Ohnishi, *Motion control systems*. Chichester, United Kingdom: Wiley & Sons, Ltd, 2011.